A Simple Tool to Measure Spasticity in Spinal Cord Injury Subjects

Arash Arami, *Member, IEEE,* Nevio L. Tagliamonte, Federica Tamburella, Hsieng-Yung, Huang, Marco Molinari and Etienne Burdet, *Member, IEEE*

***Abstract*— This work presents a wearable device and the algorithms for quantitative modelling of joint spasticity and its application in a pilot group of subjects with different levels of spinal cord injury. The device comprises light-weight instrumented handles to measure the interaction force between the subject and the physical therapist performing the tests, EMG sensors and inertial measurement units to measure muscle activity and joint kinematics. Experimental tests included the passive movement of different body segments, where the spasticity was expected, at different velocities. Tonic stretch reflex thresholds and their velocity modulation factor are computed, as a quantitative index of spasticity, by using the kinematics data at the onset of spasm detected through thresholding the EMG data. This technique was applied to two spinal cord injury subjects. The proposed method allowed the analysis of spasticity at muscle and joint levels. The obtained results are in line with the expert diagnosis and qualitative spasticity characterisation on each individual.**

I. Introduction

Spasticity is considered as a velocity-dependent increase in the tonic stretch reflexes (muscle tone with exaggerated tendon jerks), resulting from an hyperexcitability of the stretch reflex [1]. It commonly occurs after lesions in central nervous system and hinders individual's motor function recovery. Spasticity affects around 85% of subjects with multiple sclerosis, 35% of chronic hemiplegic stroke patients, and between 65 and 78% of individuals with Spinal Cord Injury (SCI) [1],[2]. It is commonly associated with clonus and spasms and adversely affects the quality of life, yield limbs stiffness and ultimately may lead to muscle shortening (contractures) and musculoskeletal deformities. These changes interfere with voluntary movements and daily functions such as ambulation, hand manipulation, balance, speech and swallowing. An increase in muscle tone or stiffness may also cause discomfort and pain, interfering with rehabilitation. Spasticity symptoms may include hypertonicity (increased muscle tone), clonus (a series of oscillating muscle contractions), exaggerated deep tendon reflexes, muscle spasms, and scissoring (involuntary crossing of the legs).

Existing clinical methods to assess the sensorimotor function are imprecise in characterising the spasticity or evaluating spasticity targeted therapy outcome. Several available clinical techniques to assess the degree of spasticity can be classified as qualitative/observational methods. These methods, which are relatively easy to implement and quick to perform, can be used in standard clinical environments without additional cost, but depend on the ability/experience of the examiner. These methods are mainly based on scales that evaluates different aspects of the pathophysiology, such as the resistance produced by muscles against passive movements (Ashworth Scale) or the frequency of spasms (Penn Spasm Frequency Scale) or the clonus (SCATS scale). However, they lack in accuracy, precision, repeatability and objectivity. The most widely used tool to assess spasticity is the Modified Ashworth Scale (MAS) [3], whose reliability depends on the examiner experience. MAS also varies with the limb, joint, and the underlying pathologies, and its inter-rater reliability is higher for the upper limb (especially wrist and elbow) than for the lower limbs [4].

These issues with current clinical estimation of spasticity motivate the use of objective quantitative methods. A quantitative model of the spasticity can be built based on the modulation of stretch reflexes thresholds [5]. Human movement and posture control lie upon the segmental and descending systems to set and reset the Spatial Threshold (ST) of reflexes, i.e. the specific muscle length or respective joint angle at which the stretch reflex and other proprioceptive reflexes begin to act [6], [5]. Based on recent findings on voluntary control of body segments [9], such as wrist motion [10], spasticity can be considered as a result of a reduction in the range of central regulation of reflex STs [8]. In a healthy subject, the range of ST regulation is defined by the task-specific ability to relax or activate muscles at any position within the biomechanical Range of Motion (RoM) of the joint. The range of possible shifts in ST may vary after a neurological disorder and result in motor deficits.

Another crucial aspect of normal motor control, also related to ST regulation, is that the ST decreases with the increase of velocity of muscle stretch [9]. This property of the neural motor control ensures the stability of posture and movement by contributing to damping and thus suppressing oscillations [10].

Recently, motorised systems were developed to study the spasticity, but such experiments are time-consuming and required complex setups [9]. In order to enhance the rehabilitation of patients suffering from spasticity and evaluate the treatments itself, a facile, accurate and objective estimation of spasticity is necessary. One possibility consists of fixing the limb to a robot controlling movement and measuring the interaction force and muscle activation. However, therapy outcomes need to be accurately evaluated

* Supported in part by the project EU-FP7 ICT-611626 (SYMBITRON: Symbiotic man-machine interactions in wearable exoskeletons to enhance mobility for paraplegics).

A. Arami, H.-Y. Huang, E. Burdet are with Human Robotics Group, Imperial College London, London, UK. e-mail: a.arami@imperial.ac.uk).

N. L. Tagliamonte, F. Tamburella, M. Molinari are with Neurorehabilitation 1 and Spinal Center, Foundation Santa Lucia, Rome, Italy (e-mail: n.tagliamonte@hsantalucia.it).

without requiring a complex, expensive and potentially dangerous experimental procedures or equipment.

In this paper, we present a simple setup we have developed for the clinical assessment of spasticity along with algorithms to accurately measure the joint kinematics, muscle activities, and examiner-subject interaction torque. This would allow obtaining quantitative estimates of the spasticity both at joint and muscle level.

II. Materials and Method

A. Sensors and Instrumentation

We developed subject-specific handles with embedded force sensors and used them with EMG sensors and Inertial Measurement Units (IMUs) to measure the interaction forces, muscles activity, and joint kinematics while moving the subject legs.

Two instrumented handles were fabricated (Fig. 1) using high-density 3D printing, each roomed with a 6 DoF force sensor (mini40 and mini45 F/T transducers, ATI Industrial Automation, USA). Two designs were provided to facilitate the interfacing to body segments with different anthropometric features. Each force sensor was connected to an amplifier and to an Analog to Digital converter for reading the data. A LabView (National Instruments, USA) GUI was used to monitor and record the applied forces. A thermoplastic layer (NC14031, Solaris, USA) was attached to the bottom part of the handle (the interface with the subject) which can be deformed while heated up to 80 ºC. This allows adapting the interface to the anatomy of each subject's segment of interest. In this paper, these handles were used to move the foot of two SCI subjects to assess ankle spasticity.

Two IMUs (MTw, Xsens, the Netherlands) were fixed on the foot and the shank which can measure the acceleration, angular velocity, and earth magnetic field, which were used to estimate each limb orientation via a Kalman filter.

EMG Trigno wireless sensors (Delsys, USA) were used, one sensor for each leg muscle which dominantly affecting the foot on sagittal plane movements (according to SENIAM recommendations): Gastrocnemius Lateralis (GL), Gastrocnemius Medialis (GM), Soleus (SOL), Tibialis Anterior (TA) and Extensor Halluces Lungus (EHL).

A Delsys trigger box was used to send a TTL square signal from the EMG system to the acquisition boards of the handles force sensors when starting and stopping each recording; data acquired by the force sensors in between the two synch pulses were considered for further analysis while the rest of data were discarded. An additional Delsys EMG sensor, with an embedded tri-axial accelerometer, was mounted on one of the IMUs; at the beginning of each test the two sensors were physically shaken together, the measured accelerations were cross-correlated during the post-processing phase to synchronise the measurements.

B. Measurement protocol and subject description

Two SCI chronic subjects were selected: S1 is female and has T10 lesion level (Ischemic) with distal motor deficits, S2 has D11-D12 lesion level (Traumatic). American Spinal Injury Association Impairment Scale (AIS) were D and A for S1 and S2 respectively. The ankle MAS scores were 2, 0, 3 and 3 for S1 left and right ankles and S2 left and right ankles respectively. The leg under investigation, i.e. the left leg, was selected based on the higher MAS score. The IMUs were attached on the dorsal part of the foot and the flat anterior medial part of the shank. The experimental setup is shown in Figure 1.

Since the angle of the adjacent joint has an effect on how bi-articular muscles are initially stretched, and consequently, on the stretch reflex thresholds and spasticity, separate tests were performed in different adjacent joint angle. Therefore, two different knee postures were considered when testing the ankle spasticity, taking into account the role of the knee on the gastrocnemius muscles (bi-articular muscles).

Functional movements, rotations dominantly around a single axis of rotation, were performed for calibration of IMUs (to align their technical frames with human anatomical frames). Calibration included the following posture and movements during which the subject maintained the supine posture:

a. A still posture with extended knee and hip and ankle at 0º with no internal-external rotation of hip or knee.

b. The examiner held their shank tightly and moved the foot for ankle plantarflexion and dorsiflexion repeatedly.

c. The examiner held the thigh of the subject and moved their shank for knee flexion/extension.

Ankle spasticity test (MAS instrumented test): The examiner moved the subject's foot with one handle to impose ankle dorsi-plantar flexion in two conditions, i.e. with the knee fully extended (KE) and then flexed (KF) at 30º (maintained with the second handle), while the patient was asked to maintain a relaxed posture. Passive dorsi-plantar flexion was performed at 5 different speeds, from the lowest to the highest, while the real-time interface of IMUs provided the speed for each trial on the screen in front of the examiner, and in the full RoM. For each speed, five trials were performed. After each passive movement test, 5s to 10s rest was allowed.

After the testing, photos from front and side were taken beside a tape meter to identify the distance between the force sensors and the joint axes of rotation in order to calculate resultant interaction torques. The presented protocol was part of a complete protocol for hip-knee-ankle spasticity evaluation approved by FSL Ethics Committee. All the patients signed an information sheet before taking part in the experiments.

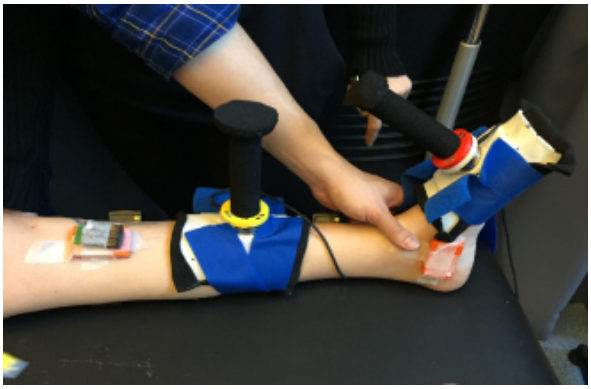

Figure 1. Experimental setup for the spasticity measurements: (a) lateral view of instrumented handles and EMG sensors, (b) medial view of handles, EMG sensors and IMUs.

C. Signal Processing and Spasticity Modelling

C.1. Pre-processing steps

Data were acquired at 256Hz for the force, EMG at 2000Hz, Delsys accelerations at 148.1Hz and IMUs at 75Hz. Data were initially synchronised based on the digital pulses given at the beginning and the end of each test and then all signals were resampled at a frequency of 75Hz.

EMG signals were band-pass filtered between 20 and 350 Hz, filtered with a notch filter at 50 Hz, full-wave rectified and finally their envelope was calculated by using a zero-lag second order Butterworth filter with a 5Hz cut-off frequency.

The body attached IMUs measured the acceleration and angular velocity in the sensor frame which was not necessarily aligned with the anatomical frame. Therefore, functional calibration steps were performed to align the frame of the sensor to the anatomical frame of each segment. Each of the functional movements, stated in II.B, allowed isolating an axis of anatomical frame measured in the sensor frame.

First, the accelerometer measurement used in the static posture to determine the gravity vector.

$$u^1_{anatomy} = [a_x\ a_y\ a_z\ |supine\ static\ posture] \quad (1)$$

where $u^1_{anatomy}$ is the gravity vector considered as the first anatomical axis, and a corresponds to the accelerometers recording. First rotation matrix was built to virtually rotate $u^1_{anatomy}$ to [0 0 1] using the Euler rotation theorem:

$$u^n = u^1_{anatomy} \times [0\ 0\ 1] \quad (2)$$

$$\theta = cos^{-1}\left(\frac{u^1_{anatomy} \cdot [0\ 0\ 1]}{\|u^1_{anatomy}\|}\right) \quad (3)$$

$$R^1 = R(u^n, \theta) \quad (4)$$

This matrix was applied to align the first axis, then singular value decomposition of rotated angular velocities was used to find the next axis:

$$UDV^T = (R^{1^T}\omega^T\omega R^1) \quad (5)$$

$$u^2_{anatomy} = U(:,1) \quad (6)$$

where D is a diagonal matrix with singular values of $\omega^T\omega$ and U and V are matrices of left and right eigenvectors. In particular, each column of U is one of the eigenvectors, and the first column, denoted by $U(:,1)$ is the eigenvector associated with the highest singular value. This eigenvector obtained during dorsi-plantar flexion represents the second anatomical axis. The second rotation matrix for each segment was obtained similarly, and the calibrated measurement of each segment is:

$$\omega_{cal} = R^2R^1\omega \quad (7)$$

The calibrated rotation matrices then applied to the measurement and fed into the Kalman filter for orientation estimation.

C.2. Spasticity modelling

Dynamic tonic stretch reflex threshold, i.e. the joint angle at which the tonic stretch reflex happens, can express quantitatively the spasticity, while this measure can be modelled as follows:

$$ST^* = ST - f(\omega) \quad (8)$$

where ST^* is the dynamic tonic stretch reflex threshold, $f(\omega)$ is a function that generates the stretch reflex dependency to the joint angular velocity, and ST is the tonic stretch reflex threshold at static condition. According to previous findings of [7], [8] a linear model for velocity dependency of stretch reflex was considered. The above equation thus leads to:

$$ST^* = ST - \mu\omega \quad (9)$$

This spasticity model is then characterized by two main measures of ST and μ. In our experiments, stretch reflex onsets defined as the filtered EMG passes a threshold of 3 times standard deviation of the rest EMG, and stay above it for at least 100 ms. Using the joint angles and angular velocities at those involuntary muscle activation onsets, we then estimate ST and μ parameters of spasticity model for the activated muscles acting on the understudy joint.

C.3. Interaction torque analysis

Torque and kinematic parameters correlation can express the presence of spastic behaviour for instance if there is an increase of correlation between the torque and joint angles.

The examiner applied forces through the two handles connected to the body segments, one to hold the adjacent segment and one to move the body segment. By using the 6 DoF load cells, forces and moments applied at each segment were estimated. Images of the segment and mounted handles against a measurement tape were used to estimate the moment arms as shown in Figures 1 and 2.

The torque at the ankle joint M_{ankle} was estimated by using equation (10). During the experiment the foot is on the air, therefore there are no ground reaction forces.

$$M_{ankle} = l_1 \times F^{foot} + l_{CoM} \times m_{foot} g + M_y^{foot} \qquad (10)$$

The absolute value of Pearson correlation coefficient between the estimated torque and kinematic measures (joint angle and angular velocity) and EMG-based features (sum of EMG activities for dorsiflexors, plantarflexors and all muscles) were computed. These correlation coefficients were computed in three different conditions:

- Baseline: during the whole experiment (including both plantar and dorsiflexion with or without muscle activations).
- ST dorsi: around the onsets of tonic stretch reflex during dorsiflexion (from 10 sample before to 10 sample after).
- ST plantar: around the onsets of tonic stretch reflex during plantarflexion (from 10 sample before to 10 sample after).

III. Results

Joint angle, angular velocity, torque and EMG measurements for a representative test on ankle dorsi-plantar flexion are depicted in Figure 3. Typical ankle angle and angular velocity at muscle reflex onsets are shown in Figure 4 for EHL (a dorsiflexor) and GL (a plantarflexor). This figure also demonstrates the fitted stretch reflex threshold model and the predicted spastic region for those muscles. The obtained parameters of the muscle-level stretch threshold models are presented in Table 1 and 2 for S1 and S2 respectively.

As expected, in S1 (MAS: 2) plantarflexors were getting spastic during the dorsiflexion, and dorsiflexors appear spastic during the plantarflexion. This is the main observation for S2 (MAS: 3) however, some extra activities were indicated. S2 also showed weak spasticity in EHL during dorsiflexion, and on GL and SOL during plantarflexion. A strong spastic behaviour observed for GM during both dorsi and plantarflexions. It can be seen for both subjects that dorsiflexors have negative ST while the plantarflexors exhibit positive ST values. In other words, the stretch reflexes during the slow dorsiflexion and plantarflexion start at slightly plantar-flexed and dorsi-flexed ankles respectively.

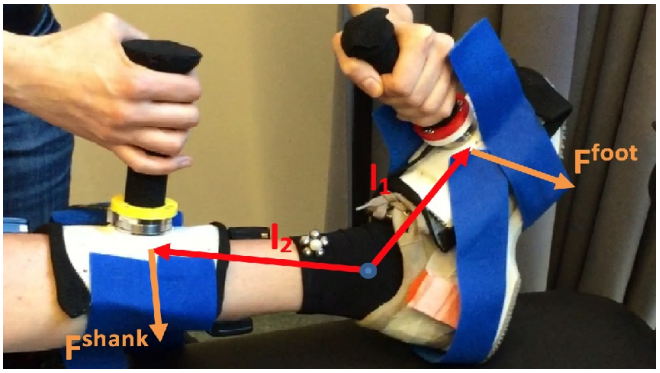

Figure 2. Handles attached to foot and leg to investigate the ankle spasticity. Interaction forces between the subject's leg and the examiner and the moment arms are also indicated. Note that during the experiment the foot was not in contact with the bed and no ground reaction force was affecting the foot.

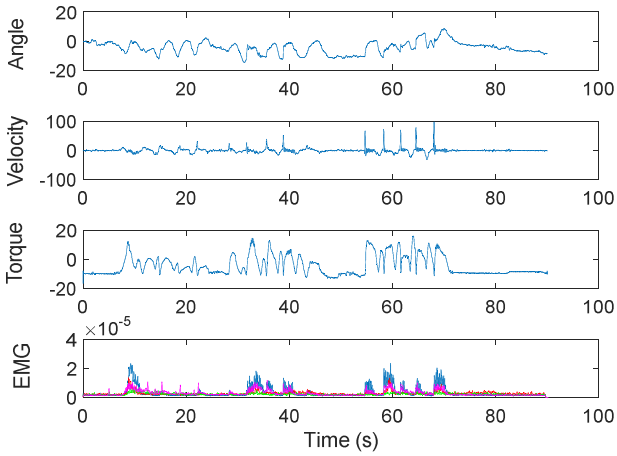

Figure 3. A representative sample of measures during spasticity test: top is ankle angle (deg); second top is the ankle angular velocity (deg/s); the third graph is a rough estimation of ankle interaction torque (Nm), and the bottom graph is the processed EMG data of ankle dorsi and plantarflexors (V).

Figure 5 depicts the intersected muscle stretch reflex threshold models (solid lines) acting on the ankle, and represents the joint-level spasticity at the ankle (the colour filled areas) for the subject S1.

Table III, IV and V report the absolute correlation between the ankle torque and angle, angular velocity, sum of EMG of dorsiflexors, the sum of EMG of plantarflexors and sum of all muscles activities, for S1 at KE condition, S2 at KE and KF conditions respectively. S1 KF condition was excluded from this analysis due to the observed random reflexes during the experiment and low R2 on Tonic stretch reflex models, particularly in the case of plantarflexors.

For both, subjects, the absolute correlation between τ and θ, indicated as $\rho(\tau,\theta)$, increased during the onsets of stretch reflexes during both dorsi and plantarflexions when compared to the baseline. The absolute correlation between the ankle torque and sum of EMG of dorsiflexors was higher than plantarflexors during the foot plantarflexion. Similarly, during the dorsiflexion, ankle torque exhibited higher correlation with EMG of plantarflexors, $\rho(\tau, \Sigma EMGplant)$, in both S1 and

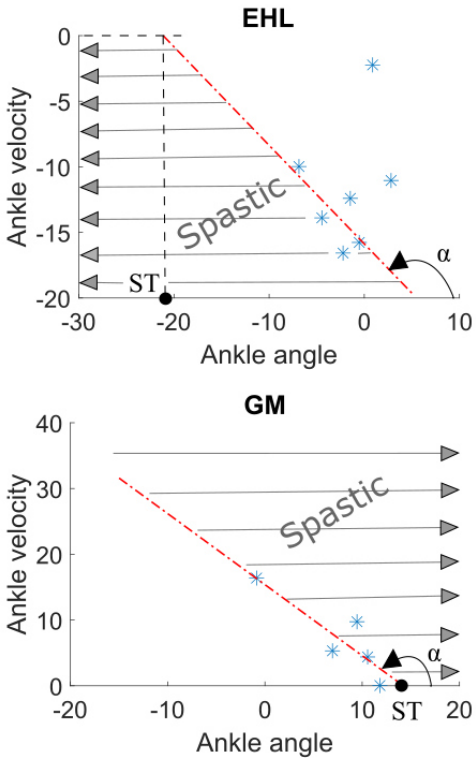

Figure 4. Spasticity model of EHL (a) as a dorsiflexor and GM (b) as a plantarflexor. The depicted light-blue data points are the measured angle and angular velocity at the onset of tonic stretch reflexes. The lines are fitted using a robust least square method and can indicate the ST (the joint angle at which the line crosses the zero velocity), and μ=-cot(α) where α is the angle between the horizontal axis and the fitted line). Gray arrows show the spastic regions.

TABLE I. S1 ANKLE SPASTICITY MODELS (MUSCLE-LEVEL DISCRIMINATION)

S1	During ankle dorsi-plantar flexion	μ	ST	R^2
TA	KE	0.53	-12.63	0.71
	KF	1.67	-14.08	0.76
EHL	KE	0.31	-1.92	0.76
	KF	1.33	-20.6	0.52
GL	KE	0.86	18.63	0.8
	KF	0.56	5.02	0.15
GM	KE	0.36	9.67	0.78
	KF	NotDefined	102.4	0.28
SOL	KE	0.42	12.61	0.95
	KF	0.60	19.67	0.1

S2 (S2 in KF condition). This can express the presence of tonic stretch reflexes, i.e. the muscles that become stretched generate some reflex tension which affects the joint torque. The increase of absolute correlation between the ankle torque and joint angle and angular velocity in the onsets of such reflexes suggests the strong dependence between those reflexes and the joint angles and angular velocity, as expected in spastic behaviours. It must be noted that the ankle torque

TABLE II. S2 ANKLE SPASTICITY MODELS (MUSCLE-LEVEL DISCRIMINATION)

S2	During ankle dorsi-plantar flexion	μ	ST	R^2
TA	KE	0.40	-28.76	0.99
	KF	0.91	-8.63	0.73
EHL	KE	2.94	-31.94	0.3
	KF	1.64	-8.89	0.6
GL	KE	0.83	13.35	0.95
	KF	5.88	92.7	0.8
GM	KE	0.93	14.27	0.78
	KF	2.78	36.39	0.18
SOL	KE	4.55	13.45	NotDefined
	KF	3.33	54.2	0.71

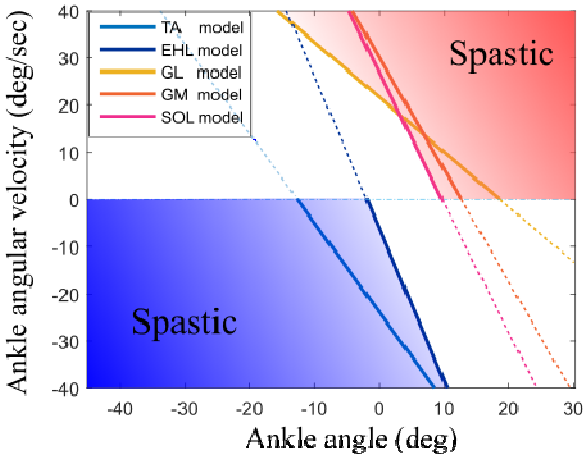

Figure 5. Ankle spastic space (S01) for the KE condition. The solid lines are the tonic stretch reflex threshold models for different muscles including dorsiflexors (TA and EHL) and plantarflexors (GL, GM and SOL). The shaded regions demonstrate the spastic behavior, where a higher degree of spasticity is expected at darker color.

and dorsiflexor EMG exhibited higher correlation for S2 even during the dorsiflexion of the foot in KF.

IV. DISCUSSION

The tonic *ST* can show the severity of spasm in each muscle while the μ represents its sensitivity to the velocity. When performing a dorsiflexion ($\omega>0$), the smaller the dorsiflexion angle at which the plantarflexor muscle activation occurs, the higher the spasticity level, which was demonstrated by small positive and even negative angle in different ankle joint velocities. Similarly, for plantar movement ($\omega<0$), the greater the angle on which the dorsiflexor muscle activation occurs, the more intense the spasticity (for instance small negative angles or even positive angles). If the *ST**s are out of the RoM, no spasticity is expected at static postures and dynamic movements respectively. The μ parameter reflects how much the stretch reflex threshold influenced by the angular velocity, a large positive μ suggests a great decrease of dynamic stretch threshold for plantarflexors as a result of higher velocity and a

TABLE III. ABSOLUTE PEARSON CORRELATION COEFFICIENTS: S1 (KE)

ρ (τ,-)	θ	ω	ΣEMG$_{dorsi}$	ΣEMG$_{plant}$	ΣEMG$_{ankle}$
Baseline	0.12	0.05	0.52	0.65	0.65
ST dorsi	0.99	0.32	0.52	0.89	0.87
ST plant	0.92	0.20	0.73	0.03	0.2

TABLE IV. ABSOLUTE PEARSON CORRELATION COEFFICIENTS: S2 (KE)

ρ (τ,-)	θ	ω	ΣEMG$_{dorsi}$	ΣEMG$_{plant}$	ΣEMG$_{ankle}$
Baseline	0.03	0.04	0.14	0.49	0.37
ST dorsi	0.38	0.63	0.26	0.02	0.19
ST plant	0.69	0.47	0.47	0.69	0.60

TABLE V. ABSOLUTE PEARSON CORRELATION COEFFICIENTS: S2 (KF)

ρ (τ,-)	θ	ω	ΣEMG$_{dorsi}$	ΣEMG$_{plant}$	ΣEMG$_{ankle}$
Baseline	0.11	0.00	0.05	0.11	0.08
ST dorsi	0.22	0.08	0.41	0.44	0.60
ST plant	0.26	0.68	0.39	0.09	0.43

great increase of stretch threshold for dorsiflexors. In this analysis of ankle spasticity performed on two subjects with SCI, the plantarflexors and dorsiflexors showed spastic behaviour when getting stretched. The *ST* and μ were estimated for dorsiflexors during the plantarflexion and the opposite for plantarflexors since they represent the reflex related to the stretching of muscles. Always positive μ represents the worsening of stretch reflex thresholds in dynamic cases, i.e. increase of this threshold for the dorsiflexors and its decrease for plantarflexors.

For S1 with the KE, among dorsiflexors, EHL was much more spastic (*ST* estimated to be close to -2 deg). While among the extensors GM was the most spastic one (*ST* less than 10 deg). Flexing the knee dominantly affect the biarticular plantarflexors. This was attributed to the decrease of linear fit R^2 advocating the weakening of the joint angle and angular velocity at the reflexes. During foot movement at KF condition, GM did not exhibit spasticity with an *ST* estimate out of the RoM with almost no dependency on angular velocity. This is reasonable since the knee was flexed and the biarticular plantarflexors were less stretched.

For S2, when flexing the knee the ankle plantarflexors became more relaxed, ST increased drastically and shifted out of the RoM. Also a decrease in μ parameters observed for the plantarflexors. The increase of *ST* and decrease of μ corroborate to the fact that S2 would not experience spasm on plantarflexors when the knee is flexed particularly in slow movements. While this decrease of tonic stretch reflexes is evident for GL and GM, i.e. biarticular muscles, the decrease of spasticity in SOL is not. SOL is a mono-articular muscle and such behaviour needs to be investigated with more scrutiny.

The μ values were always positive for all muscles and both subjects. The most sensitive stretch reflexes to velocities appeared in TA and GL for S1 and EHL and SOL for S2 when performing the test in KE. Some of the S2 muscles are more than twice sensitive to change of velocity ($\mu^{S2} >> \mu^{S1}$) which indicates this subject to show more spasticity during movement and dynamic ankle rotations. Flexing the knee showed different results in the μ parameters. In S1, flexing the knee increased the μ of TA and EHL while decreased the μ of GL. This suggests that dorsiflexors tonic stretch reflexes become more sensitive to velocity when the knee is flexed. This finding is not evident from the musculoskeletal model; those muscles lengths are less affected by the knee angle. More investigation is thus required to explain such alternations. In S2, the sensitivity of stretch reflex was decreased for dorsiflexors when flexing the knee, while in the plantarflexor muscles μ increased for GL and GM and SOL. While this change for GL and GM is evident, the length of SOL, as a mono-articular muscle acting on the ankle, should not depend on the knee angle. Plantarflexors and dorsiflexors exhibited reflexes in S2 even when the muscles were not stretching. While at first glance the presence of reflex when the muscle is shortening might seem against the tonic stretch reflex threshold theorem, it may account for muscle co-contraction of and clonus which are common in spastic subjects (e.g. S2).

The absolute correlation between ankle interaction torque and both ankle dorsiflexion angle and angular velocity were much higher in the proximity of the tonic stretch reflex onsets than the whole experiment (baseline). This reflects the presence of a resistive torque which depends on the muscle length and its rate of change which manifested the presence of spasticity. In both subjects the aggregated EMG of dorsiflexors showed a higher correlation with the estimated torque during the plantarflexion then dorsiflexion, except in the case of S2 with KF, where the correlation coefficients are close for the both movements. The plantarflexors aggregated EMG correlation with torque increased during muscle onsets at dorsiflexion (except the KE condition in S2).

V. CONCLUSION

This work presented a novel and easy-to-use device and algorithms for quantitative evaluation of spasticity in the clinical environment. The device consists of two instrumented handles embedding 6 DoF load cells, IMUs and EMG sensors to measure the interaction torques, joint kinematics, and muscle activation respectively. Spasticity was quantified first at the muscle level using linear tonic stretch reflex threshold models. These models represent the relationship between joint angular velocity and the joint angle at the onsets of reflex for each specific muscle. The aggregation of those stretch reflex threshold models then resulted in a joint spasticity model that indicated in which joint subspaces the spastic behaviour was expected. Finally, a torque correlation analysis was done to validate the resultant spastic models. In contrast to the existing clinical tests for spasticity such as MAS, the proposed technique provided an objective evaluation tool. In comparison with a few existing robotic-based studies, the proposed technique is facile and has the potential to be transferred to the clinical environment.

A larger population of SCI subjects will be recruited and the proposed method will be compared with the clinical scores

in future. Different spastic characteristics were expected in different subjects as they present non-homogeneous neurological and clinical conditions. The proposed method provides subject-specific modelling of the spasticity and can mark the spastic regions in the joint space. This will enable the design of a control layer for assistive exoskeleton controllers, such as [11], in order to modify the gait trajectory of the user to avoid the spastic regime. This design can provide a spasm-free wearable exoskeleton and contribute in the design of a controller tailored to each individual neurophysiological characteristics.

REFERENCES

[1] F. M. Maynard, R. S. Karunas, and W. P. Waring, 'Epidemiology of spasticity following traumatic spinal cord injury', Arch. Phys. Med. Rehabil., vol. 71, no. 8, pp. 566–569, Jul. 1990.

[2] D. K. Sommerfeld, E. U.-B. Eek, A.-K. Svensson, L. W. Holmqvist, and M. H. von Arbin, 'Spasticity after stroke: its occurrence and association with motor impairments and activity limitations', Stroke, vol. 35, no. 1, pp. 134–139, Jan. 2004.

[3] A. D. Pandyan, P. Vuadens, F. M. J. van Wijck, S. Stark, G. R. Johnson, and M. P. Barnes, 'Are we underestimating the clinical efficacy of botulinum toxin (type A)? Quantifying changes in spasticity, strength and upper limb function after injections of Botox to the elbow flexors in a unilateral stroke population', Clin. Rehabil., vol. 16, no. 6, pp. 654–660, Sep. 2002.

[4] A. D. Pandyan, G. R. Johnson, C. I. Price, R. H. Curless, M. P. Barnes, and H. Rodgers, 'A review of the properties and limitations of the Ashworth and modified Ashworth Scales as measures of spasticity', Clin. Rehabil., vol. 13, no. 5, pp. 373–383, Oct. 1999.

[5] M. L. Latash, Fundamentals of Motor Control. Academic Press, 2012.

[6] A. G. Feldman, 'Space and time in the context of equilibrium-point theory', Wiley Interdiscip. Rev. Cogn. Sci., vol. 2, no. 3, pp. 287–304, May 2011.

[7] H. Raptis, L. Burtet, R. Forget, and A. G. Feldman, 'Control of wrist position and muscle relaxation by shifting spatial frames of reference for motoneuronal recruitment: possible involvement of corticospinal pathways', J. Physiol., vol. 588, no. Pt 9, pp. 1551–1570, May 2010.

[8] A. A. Mullick, N. K. Musampa, A. G. Feldman, and M. F. Levin, 'Stretch reflex spatial threshold measure discriminates between spasticity and rigidity', Clin. Neurophysiol. Off. J. Int. Fed. Clin. Neurophysiol., vol. 124, no. 4, pp. 740–751, Apr. 2013.

[9] M. F. Levin, R. W. Selles, M. H. G. Verheul, and O. G. Meijer, 'Deficits in the coordination of agonist and antagonist muscles in stroke patients: implications for normal motor control', Brain Res., vol. 853, no. 2, pp. 352–369, Jan. 2000.

[10] J.-F. Pilon and A. G. Feldman, 'Threshold control of motor actions prevents destabilizing effects of proprioceptive delays', Exp. Brain Res., vol. 174, no. 2, pp. 229–239, Sep. 2006.

[11] F. Dzeladini, A.R. Wu, D. Renjewski, A. Arami, E. Burdet, E. van Asseldonk, H. van der Kooij, A. Ijspeert, "Effects of a Neuromuscular Controller on a Powered Ankle Exoskeleton During Human Walking," 6th IEEE Int. conf. biomedical robotics, biomechatronics (BioRob), Singapore, pp. 617-622, June 2016.